

***Pseudomonas aeruginosa* infection augments inflammation through miR-301b repression of c-Myb-mediated immune activation and infiltration**

Xuefeng Li^{1,2#}, Sisi He^{1,2#}, Rongpeng Li^{1#}, Xikun Zhou^{1,2#}, Shuang Zhang^{1,2}, Min Yu^{1,3}, Yan Ye¹, Yongsheng Wang², Canhua Huang^{2*}, and Min Wu^{1*}

¹Department of Biomedical Sciences, University of North Dakota, Grand Forks, North Dakota, 58203-9037, USA;

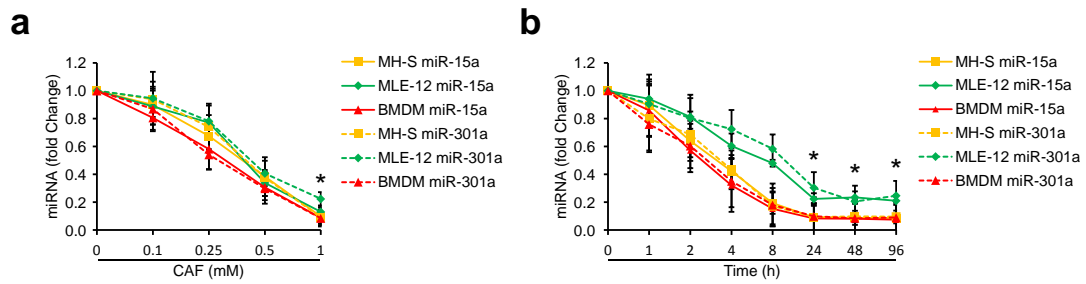
²State Key Laboratory of Biotherapy and Cancer Center, West China Hospital, Sichuan University, and Collaborative Innovation Center for Biotherapy, Chengdu, 610041, P. R. China;

³Department of Thoracic Oncology, West China Hospital, Sichuan University, Chengdu, 610041, P.R. China.

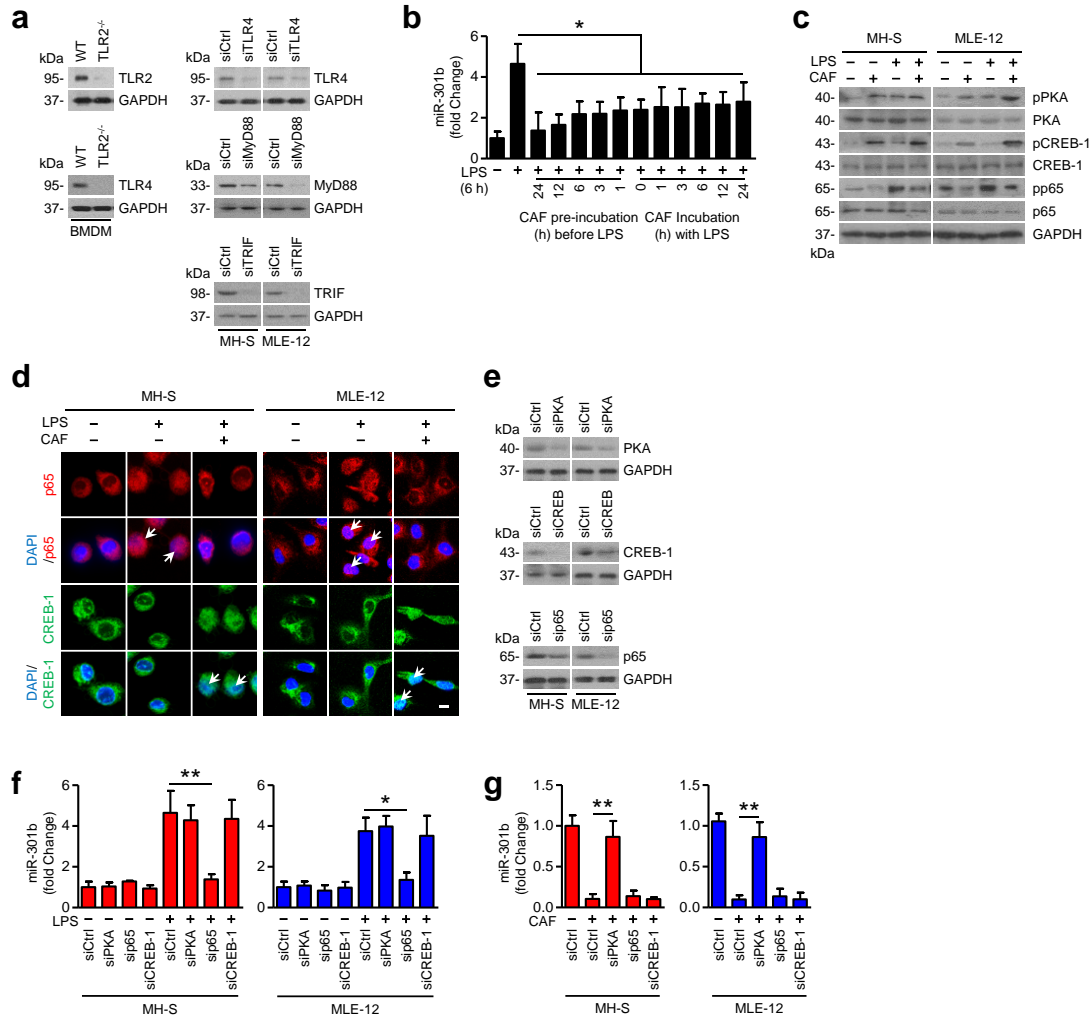
*Corresponding author: Min Wu, E-mail: min.wu@med.und.edu, Tel: +01-(701)777-4875; Fax: +01-(701)777-2382; or Canhua Huang, E-mail: hcanhua@hotmail.com, Tel: +86-13258370346, Fax: +86-28-85164060.

#These authors contributed equally to this work.

Supplementary Figures and Figure Legends:

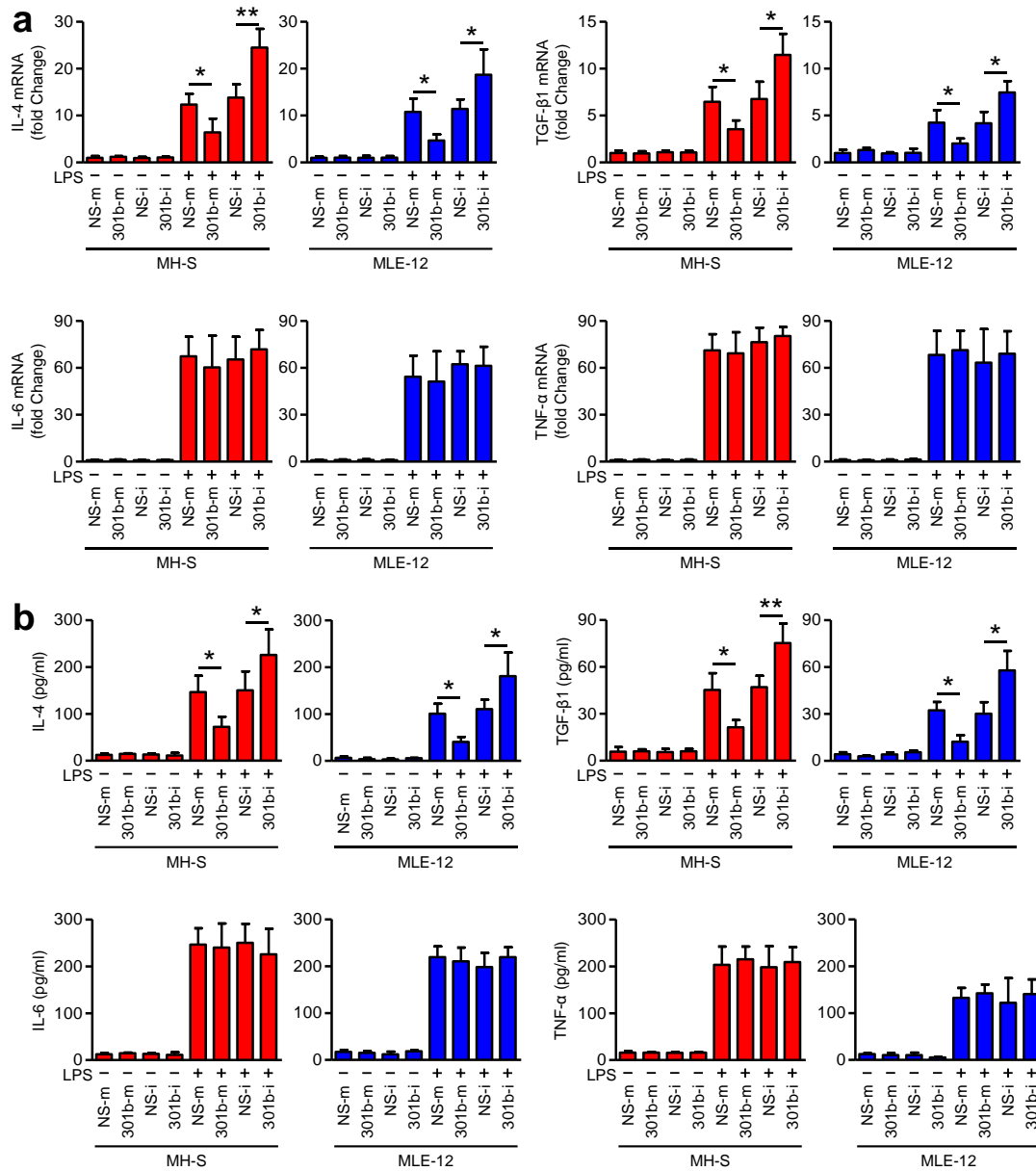


Supplementary Fig. 1. Analysis of miRNA expressions with CAF treatment. (a) MH-S, MLE-12, and BMDM cells were treated with CAF (1 mM, 24 h). qRT-PCR validation of miR-15a and miR-301a expressions in cells treated with different dose of CAF (24 h). (b) qRT-PCR validation of miR-15a and miR-301a expressions in cells after CAF treatment (1 mM) for various times. Data are shown as means \pm SD from triplicate. *, $p < 0.05$. One-way ANOVA with Tukey's post hoc.

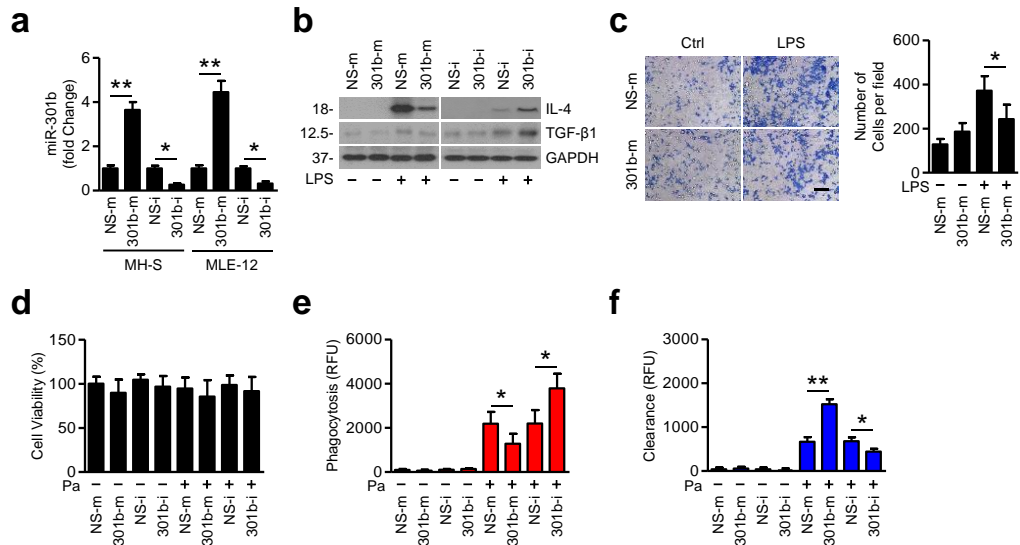


Supplementary Fig. 2. LPS induces miR-301b via TLR4/MyD88/NF-κB signaling.

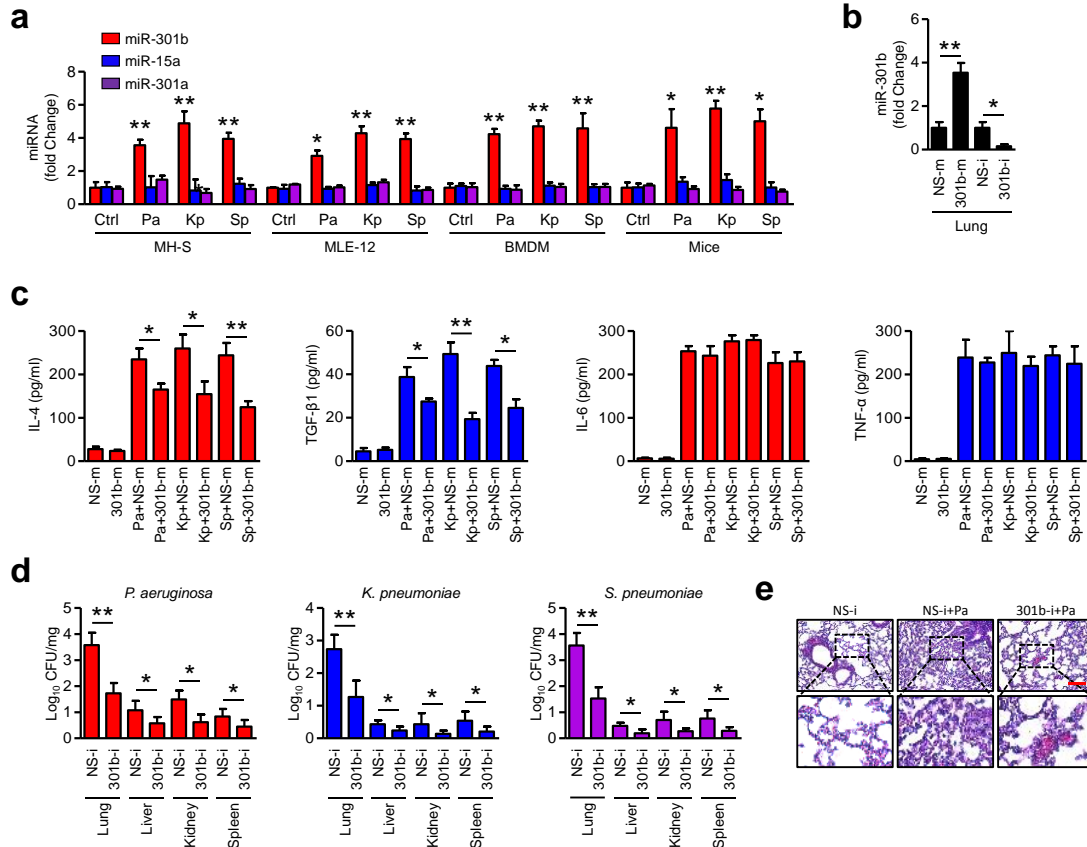
(a) Western blotting showing knockout of TLR2 and TLR4 in BMDM from WT, TLR2^{-/-} or TLR4^{-/-} mice. The right panels show the interference efficiency by TLR4, MyD88 or TRIF siRNA in MH-S and MLE-12 cells. (b) MH-S cells were incubated with CAF (1 mM). At indicated times, LPS (100 ng/ml) were added to induce miR-301b determined by qRT-PCR. (c) Protein lysates from MH-S and MLE-12 cells were analyzed for (p)PKA, (p)CREB-1 or (p)p65 expression by western blotting. After CAF pretreatment for 24 h, LPS (100 ng/ml) were added for another 6 h to induce miR-301b. (d) Immunostaining by confocal imaging in MH-S and MLE-12 cells treated as above showing nuclear translocation of p65 or CREB-1, respectively. Scale bar=10 μm. Arrows point to protein nuclear translocation. (e) Western blotting showing siRNA knockdown of PKA, CREB and p65 in MH-S and MLE-12 cells. (f, g) After siRNA interference, cells were treated with LPS (100 ng/ml, 6 h) (f) or CAF (1 mM, 24 h) (g) and miR-301b was analyzed by qRT-PCR. Panel a, c, d, e, data are representative of 3 independent experiments; b, f, g, means+SD from triplicate. *, $p < 0.05$, **, $p < 0.01$. One-way ANOVA with Tukey's post hoc.



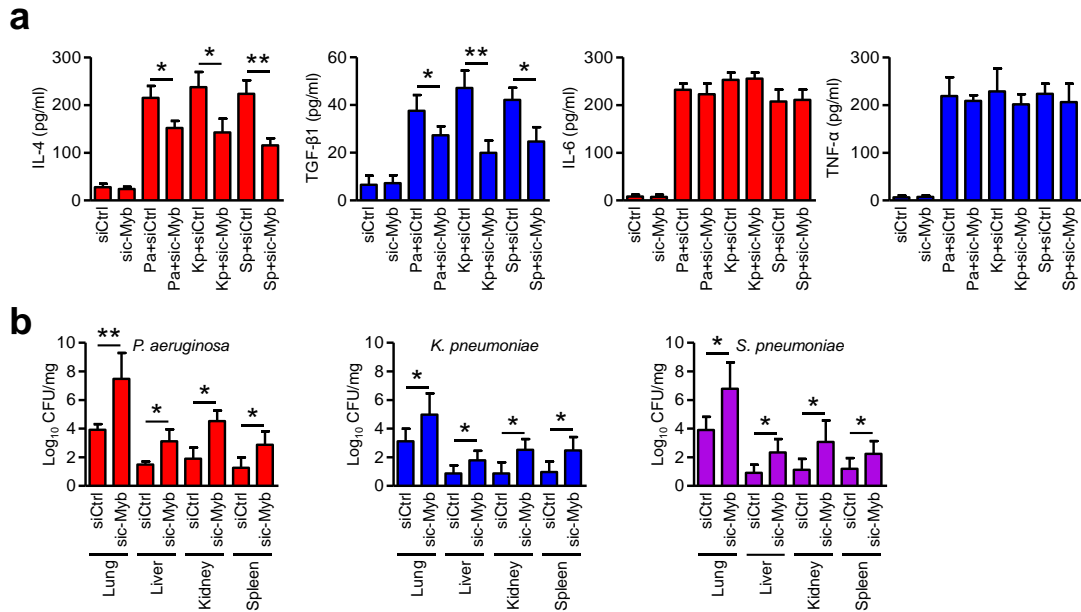
Supplementary Fig. 3. miR-301b inhibits LPS-induced anti-inflammatory cytokine *in vitro*. MH-S and MLE-12 cells were transfected with miRNA-negative control (NS-m) or miR-301b mimics (301b-m), miRNA inhibitor negative control (NS-i) or miR-301b inhibitor (301b-i), respectively. 24 h later, transfection efficiencies were detected by qRT-PCR (Supplementary Fig. 4a) and then treated with LPS (100 ng/ml, 6 h). (a) mRNA was extracted to measure inflammatory cytokines by qRT-PCR. (b) Cell culture supernatants from above were assessed for cytokine secretion by ELISA. All data are shown as means+SD from triplicate. *, $p < 0.05$, **, $p < 0.01$. One-way ANOVA with Tukey's post hoc.



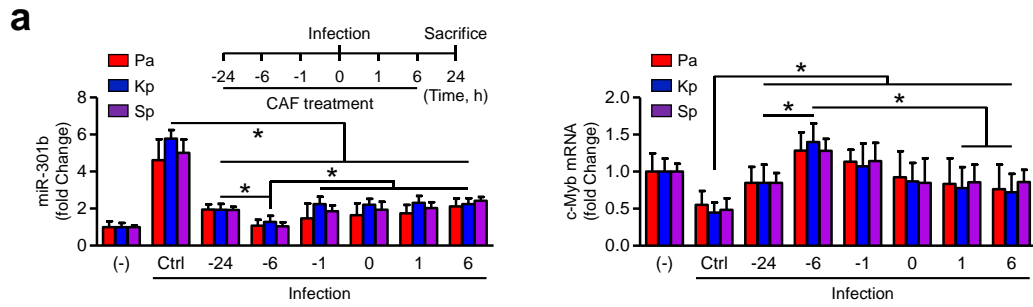
Supplementary Fig. 4. miR-301b down-regulates anti-inflammatory cytokines as well as macrophage activities. (a) MH-S and MLE-12 cells were transfected with miRNA-negative control (NS-m) or miR-301b mimics (301b-m), miRNA inhibitor negative control (NS-i) or miR-301b inhibitor (301b-i) for 24 h, respectively. The transfection efficiency was determined by checking the miR-301b levels using qRT-PCR. (b) After transfection as above, MLE-12 cells were treated with LPS (100 ng/ml, 6 h). Cells were lysed for immunoblotting to detect IL-4 and TGF-β1 protein. (c) Transwell assay for MH-S cells plated on the upper cell culture inserts, with culture medium from MLE-12 cells transfected as above in the lower chambers. Scale bars=100 μm. (d) MH-S cells were transfected as above. After transfection, cells were infected with PAO1-GFP (MOI=10, 1 h). Proliferative ability was measured by MTT assay. (e) Fluorescence intensity was calculated to measure phagocytosis 1 h after PAO1-GFP infection. (f) Bacterial clearance ability was determined by reading fluorescence intensity after overnight. Panel a, d-f, means+SD from triplicate; b, c, representative of 3 independent experiments. *, $p < 0.05$, **, $p < 0.01$. One-way ANOVA with Tukey's post hoc.



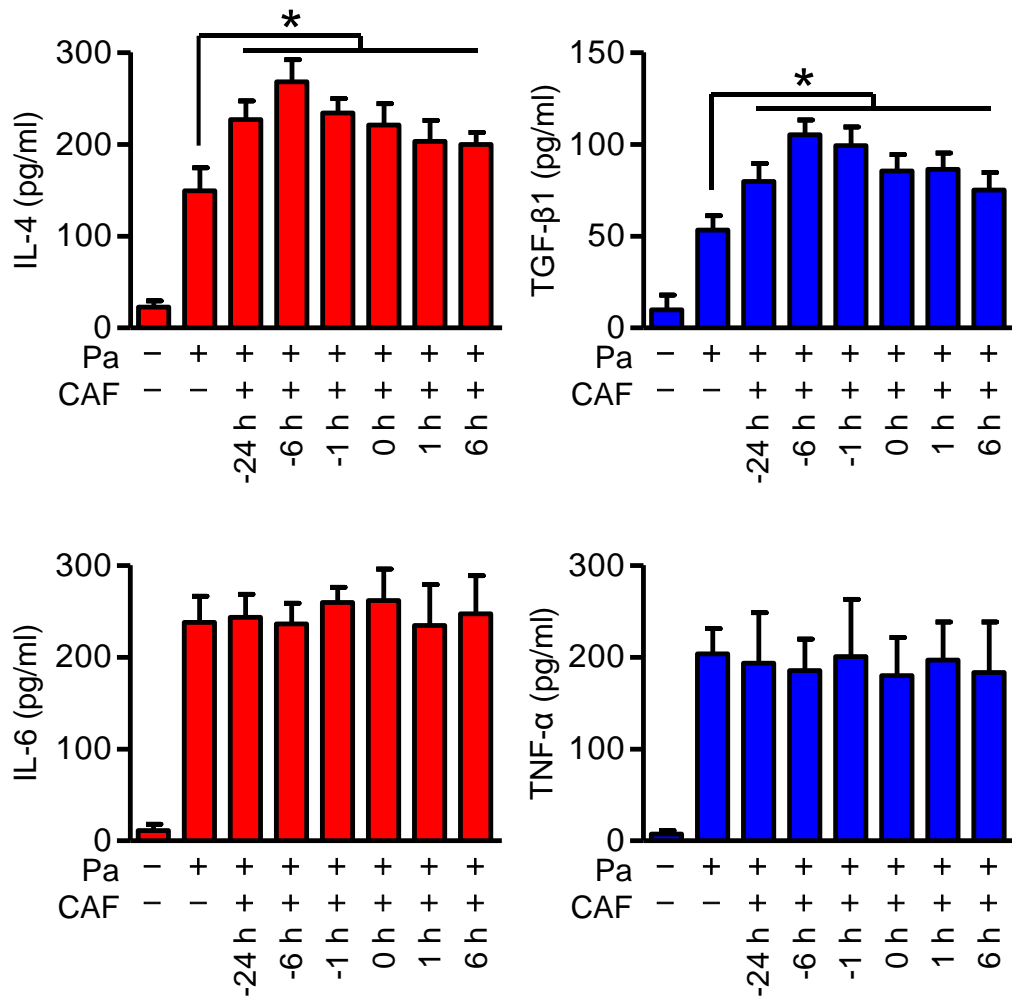
Supplementary Fig. 5. *In vivo* validation of miR-301b's function. (a) MH-S, MLE-12, and BMDM cells were infected with Pa, Kp or Sp (MOI=10, 1 h). Mice (n=3) infected with Pa (1×10^7 CFU), Kp (1×10^5 CFU), Sp (5×10^6 CFU). The expression of miR-301b, 15a and 301a was determined using qRT-PCR. (b) Mice were *i.v.* injected with NS-m, 301b-m, NS-i or 301b-i (50 μ g/mouse, n=3, 24 h). Lungs were collected for the transfection efficiency validation. (c) BAL fluids from mice (n=3) treated as above were assessed for cytokines by ELISA. (d) Organs were collected from mice (n=3) and homogenized for CFU assay. (e) Representative data of lungs (from mice transfected as above and then infected with Pa, n=3) were embedded in formalin and sections were stained by H&E. Scale bar=100 μ m. Insets showing the typical tissue injury and inflammatory influx. Panel a-d, means+SD. *, $p < 0.05$, **, $p < 0.01$. One-way ANOVA with Tukey's post hoc.



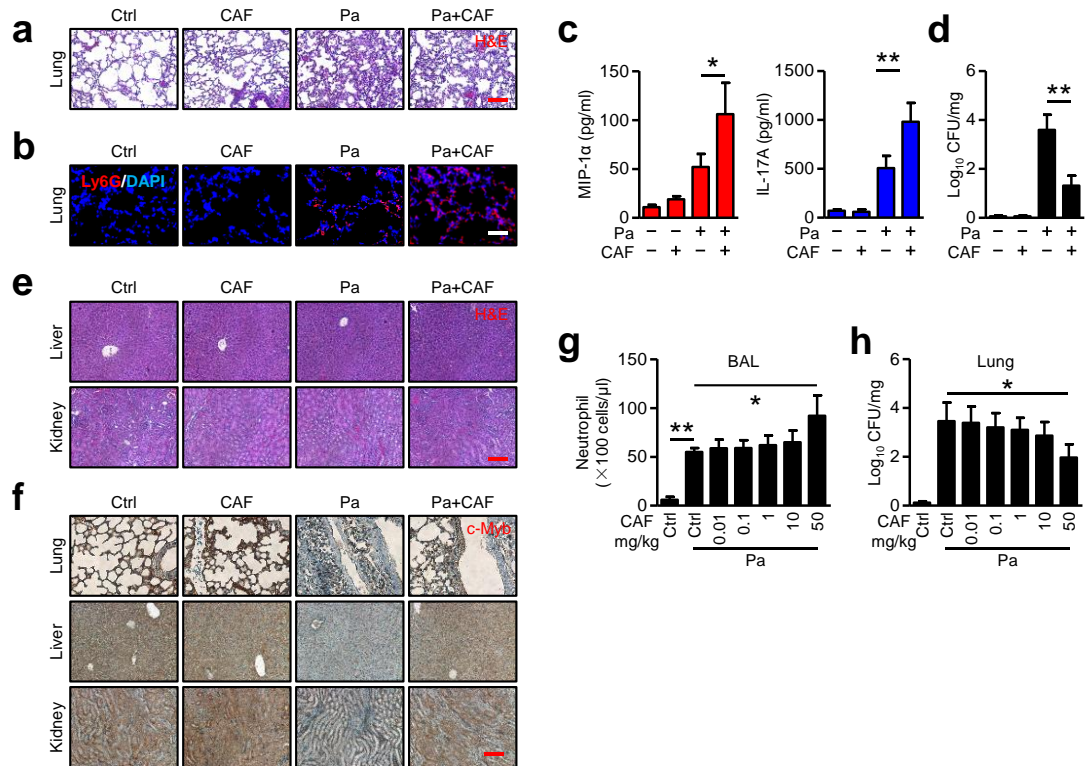
Supplementary Fig. 6. c-Myb participated the regulation of inflammatory responses. (a) Mice (n=3) were i.v. injected with Ctrl siRNA or c-Myb siRNA (50 μ g/mouse, 24 h) and were infected with Pa (1×10^7 CFU), Kp (1×10^5 CFU) or Sp (5×10^6 CFU) for 24 h. Cytokine secretion in BAL fluids was determined by ELISA. (b) Organs from mice (n=3) treated as above were homogenized for CFU assays. Panel a, b, means+SD from triplicate. *, $p < 0.05$, **, $p < 0.01$. One-way ANOVA with Tukey's post hoc.



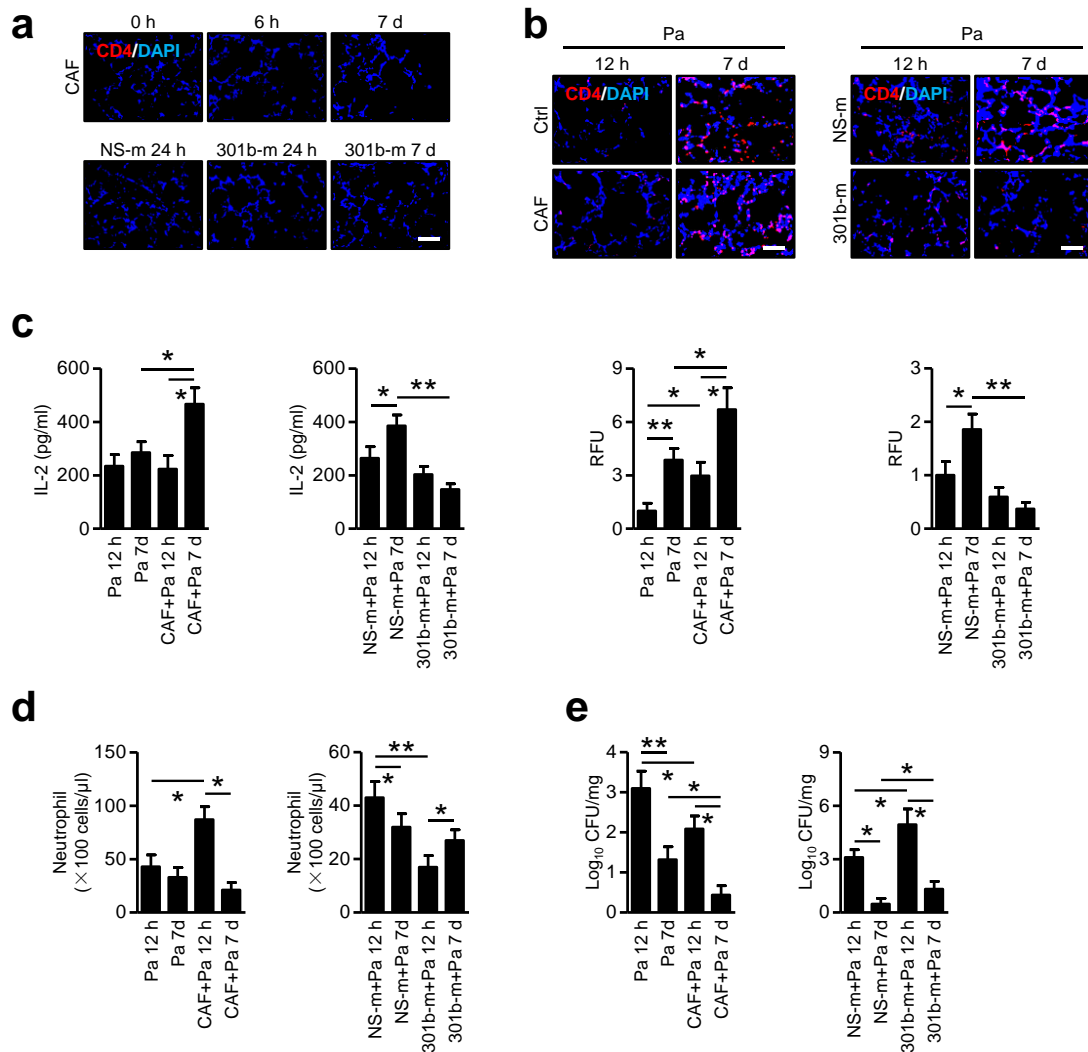
Supplementary Fig. 7. Different treatment strategy of CAF modulates infectious process *in vivo*. (a) Mice (n=3) were infected with *Pa* (1×10^7 CFU), *Kp* (1×10^5 CFU) or *Sp* (5×10^6 CFU) for 24 h. CAF (50 mg/kg, *i.v.*) was injected at indicated times (pre-treatment strategy or post-infection treatment). qRT-PCR determined miR-301b and c-Myb expression. Means+SD from triplicates. *, $p < 0.05$. One-way ANOVA with Tukey's post hoc.

a

Supplementary Fig. 9. Different treatment time of CAF modulates Pa infection. (a) Mice (n=3) were infected with Pa (1×10^7 CFU) for 24 h. CAF (50 mg/kg, i.v.) was injected at indicated time (pre-treatment strategy or post-infection treatment). BAL fluids from mice above were assayed by ELISA to measure cytokine secretion. Means+SD from triplicates. *, $p < 0.05$. One-way ANOVA with Tukey's post hoc.

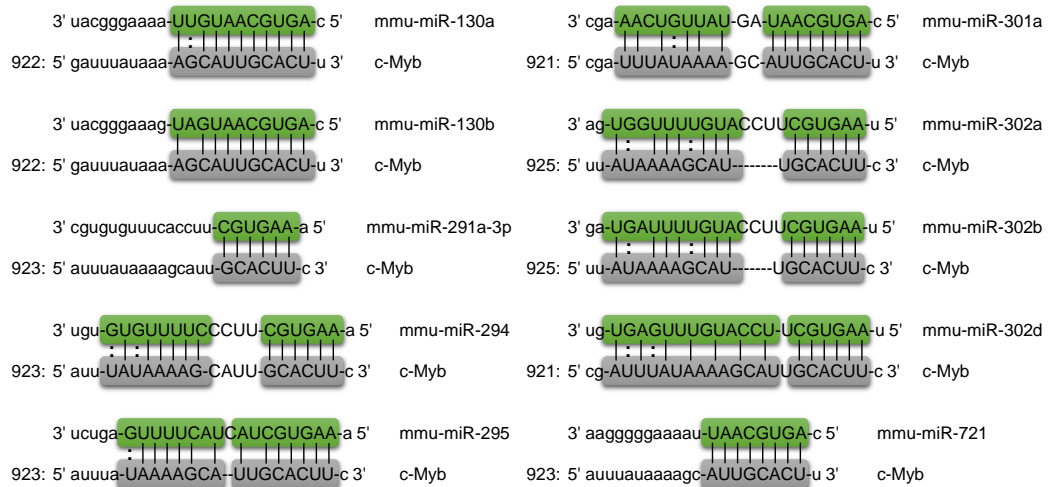


Supplementary Fig. 10. CAF suppresses inflammatory response against Pa infection *in vivo*. Mice (n=3) were treated with CAF (50 mg/kg, *i.v.*, 6 h before infection), and the mice were then infected with Pa (1×10^7 CFU, 24 h). (a) Lung tissue injury assessed by histological analysis. The lungs were paraffin-embedded and sections were analyzed by H&E staining. Scale bar=100 μ m. (b) Lungs were also evaluated by immunostaining with Ly6G antibody neutrophil infiltration. Scale bar=50 μ m. (c) After treatment as above, ELISA was performed to evaluate MIP-1 α and IL-17A levels in BAL. (d) Lung homogenates were used for CFU assays to determine bacterial burdens after CAF treatment as above. (e) Liver and kidney tissue injury assessed by histological analysis. The tissues were paraffin-embedded and sections were analyzed by H&E staining. Scale bar=100 μ m. (f) Lung, liver and kidney were also used for immunohistochemistry for c-Myb protein detection. Scale bar=100 μ m. (g, h) Mice were treated with different dosage of CAF (*i.v.*, 6 h before infection) as above, and the mice were then infected with Pa (1×10^7 CFU, 24 h). Neutrophils numbers in BAL were counted by H&E staining and bacterial burdens in lungs were counted using CFU assays. Panel a, b, e-h, representative from 3 mice; c, d, means+SD from 3 mice. *, $p < 0.05$, **, $p < 0.01$. One-way ANOVA with Tukey's post hoc.

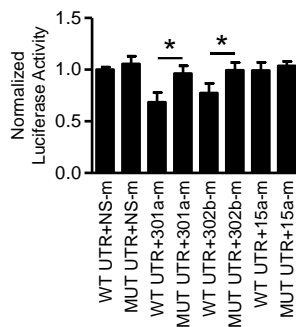


Supplementary Fig. 11. CAF and miR-301b manipulation affects the adaptive immunity. (a) Mice were pretreated with CAF or NS-m, 301b-m as above for indicated times. Lungs were collected and sectioned for immunostaining with CD4 antibody. Scale bar=50 μ m. (b) Mice were pretreated with CAF or NS-m, 301b-m for 24 h. Then mice were infected with PAO1 (1×10^5 CFU) for 12 h or 7 d, and lungs were collected and sectioned for immunostaining with CD4 antibody. Immunofluorescence scores were shown and compared. Scale bar=50 μ m. (c) IL-2 levels in BAL from above were determined using ELISA. (d) Neutrophils in BAL were counted by H&E staining. (e) Bacterial burdens in lungs were counted using CFU assays. Panel a, b, representative from 3 mice; c-e, means+SD from 3 mice. *, $p < 0.05$, **, $p < 0.01$. One-way ANOVA with Tukey's post hoc.

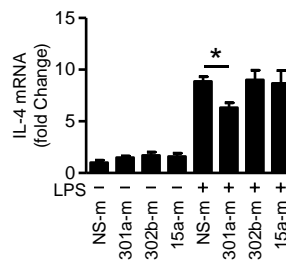
a



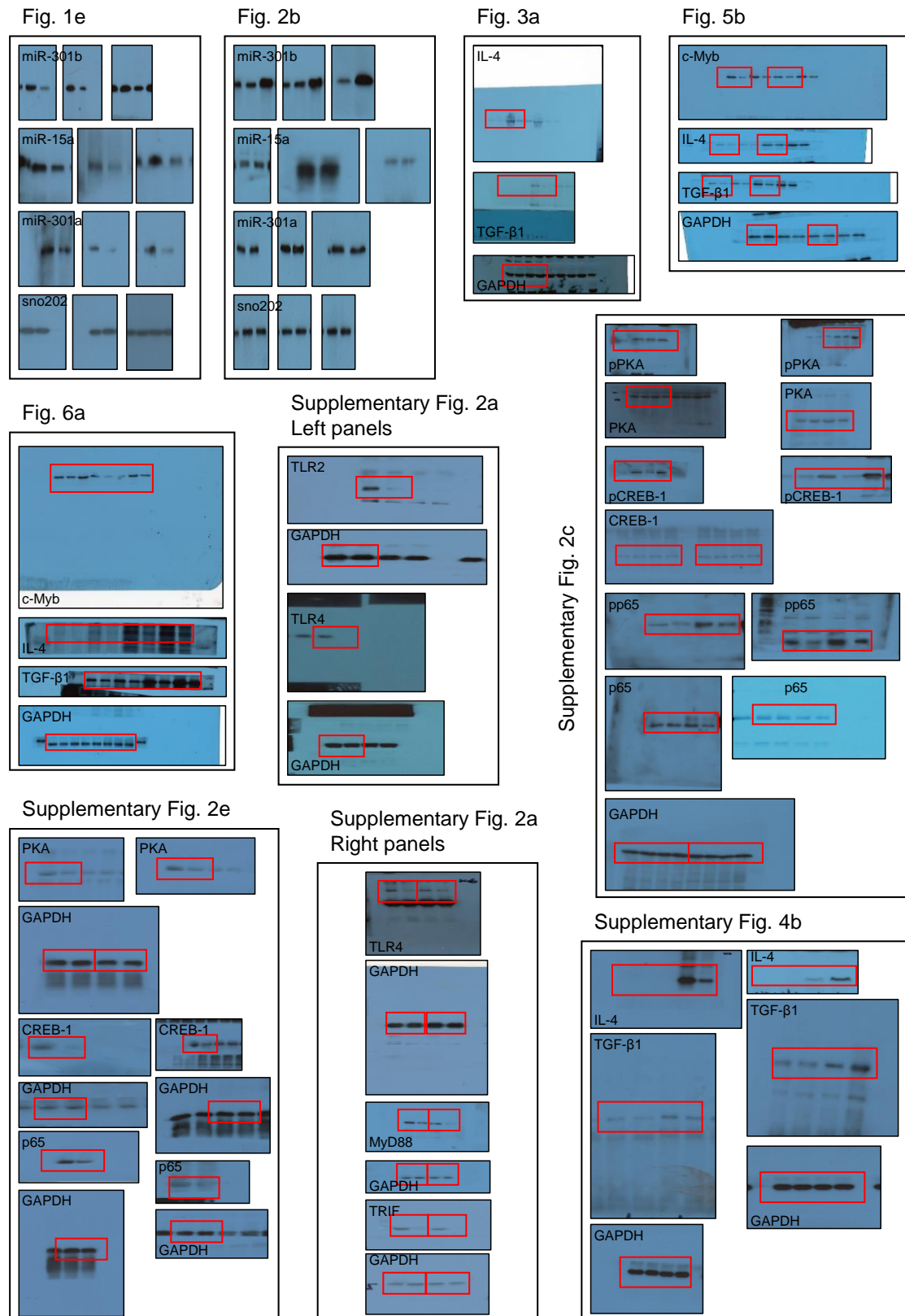
b



c



Supplementary Fig. 12. Predicated miRNAs that target c-Myb (sites: 921-943). (a) The site that is targeted by miR-301b in c-Myb 3'UTR could also be targeted by other 10 miRNAs. (b) MLE-12 cells were co-transfected with WT or mutated 3'UTR reporter constructs for NS-m, 301a-m, 302b-m or 15a-m for 24 h, respectively. Luciferase reporter assay was performed to determine the binding inhibition of miRNA. (c) IL-4 mRNA expressions in above samples were also determined by qRT-PCR. Panel b, c, means+SD from triplicate. *, $p < 0.05$. One-way ANOVA with Tukey's post hoc.



Supplementary Fig. 13. Uncropped Northern and Western blots. Frame indicate lanes that were used in figures.

Supplementary Table 1. Micro Array data of miRNAs that were regulated upon CAF treatment. The array was performed once and the values were reported without standard errors

Mature ID	Fold Regulation
mmu-let-7a-5p	-1.8636
mmu-let-7b-5p	-2.7832
mmu-let-7c-5p	-1.0874
mmu-let-7d-5p	-1.8272
mmu-let-7e-5p	1.0458
mmu-let-7f-5p	-2.8147
mmu-let-7g-5p	-1.548
mmu-let-7i-5p	-4.2175
mmu-miR-106a-5p	-1.9325
mmu-miR-106b-5p	-6.0122
mmu-miR-1192	5.2377
mmu-miR-126a-5p	1.0088
mmu-miR-128-3p	-1.1321
mmu-miR-130a-3p	4.5706
mmu-miR-130b-3p	-1.6201
mmu-miR-135a-5p	5.2377
mmu-miR-140-5p	-3.3007
mmu-miR-144-3p	5.2377
mmu-miR-155-5p	2.3496
mmu-miR-15a-5p	-10.3318
mmu-miR-15b-5p	-2.2938
mmu-miR-16-5p	-1.6584
mmu-miR-17-5p	-3.212
mmu-miR-181a-5p	-1.2872
mmu-miR-181b-5p	1.2832
mmu-miR-181c-5p	-2.107
mmu-miR-181d-5p	2.2955
mmu-miR-182-5p	5.2377
mmu-miR-186-5p	-2.7955
mmu-miR-195a-5p	-1.9347
mmu-miR-19a-3p	-3.7998
mmu-miR-19b-3p	-3.1175
mmu-miR-200c-3p	2.1644
mmu-miR-20a-5p	-3.2883
mmu-miR-20b-5p	-3.1017
mmu-miR-221-3p	-1.7915
mmu-miR-222-3p	-1.6782
mmu-miR-23a-3p	1.2701

mmu-miR-23b-3p	1.8144
mmu-miR-26a-5p	1.3929
mmu-miR-26b-5p	-1.9199
mmu-miR-27a-3p	-1.8825
mmu-miR-27b-3p	-1.3834
mmu-miR-291a-3p	2.5629
mmu-miR-294-3p	5.2377
mmu-miR-295-3p	5.2377
mmu-miR-29a-3p	-2.2409
mmu-miR-29b-3p	-3.1571
mmu-miR-29c-3p	-2.8087
mmu-miR-301a-3p	-11.0764
mmu-miR-301b-3p	-10.822
mmu-miR-302b-3p	5.2377
mmu-miR-302d-3p	5.2377
mmu-miR-30a-5p	-1.5731
mmu-miR-30b-5p	-1.525
mmu-miR-30c-5p	1.8895
mmu-miR-30d-5p	1.5224
mmu-miR-30e-5p	-2.4303
mmu-miR-322-5p	-2.8729
mmu-miR-325-3p	5.2377
mmu-miR-338-5p	2.8168
mmu-miR-340-5p	-4.718
mmu-miR-350-3p	-1.1707
mmu-miR-369-3p	5.2377
mmu-miR-384-5p	5.2377
mmu-miR-410-3p	3.1199
mmu-miR-429-3p	-1.3796
mmu-miR-466d-3p	5.2377
mmu-miR-466k	5.2377
mmu-miR-495-3p	6.1257
mmu-miR-497-5p	-4.3209
mmu-miR-568	5.2377
mmu-miR-590-3p	5.2377
mmu-miR-669h-3p	1.2455
mmu-miR-669k-3p	1.2177
mmu-miR-694	4.4891
mmu-miR-712-5p	1.2883
mmu-miR-721	5.2377
mmu-miR-743a-3p	5.2377
mmu-miR-743b-3p	5.2377
mmu-miR-876-3p	5.2377

mmu-miR-9-5p	1.6827
mmu-miR-93-5p	-2.7911
mmu-miR-98-5p	-1.3406

Supplementary Table 2. Primers designed for miRNA and mRNA determination by qRT-PCR.

ID	Primer Sequences (5'-3')
mmu-miR-301a-3p Sense	CGGCGCAGTGCAATAGTATTGTCAAAGC
mmu-miR-301b-3p Sense	CGGCGCAGTGCAATGGTATTGTCAA
mmu-miR-15a-5p Sense	GTAGCAGCACATAATGGTTTGTG
mmu-snoRNA202 Sense	GCCTTTTGAACCCTTTTCCATCTG
mmu-c-Myb Sense	TTTTCACCTAGCCAGCAGCC
mmu-c-Myb Antisense	CGCCTTTTTCGTAGGACGAC
mmu-IL-4 Sense	ACCCCAGCTAGTTGTCATC
mmu-IL-4 Antisense	TCGTTGCTGTGAGGACGTTT
mmu-IL-10 Sense	TAACTGCACCCACTTCCCAG
mmu-IL-10 Antisense	AAGGCTTGGCAACCCAAGTA
mmu-TGF- β 1 Sense	AGCTGCGCTTGCAGAGATTA
mmu-TGF- β 1 Antisense	AGCCCTGTATTCCGTCTCCT
mmu-IL-1 β Sense	GTCAACGTGTGGGGGATGAA
mmu-IL-1 β Antisense	AAGCAATGTGCTGGTGCTTC
mmu-IL-6 Sense	CCCCAATTTCCAATGCTCTCC
mmu-IL-6 Antisense	CGCACTAGGTTTGCCGAGTA
mmu-TNF- α Sense	GGCAGGTTCTGTCCCTTTCA
mmu-TNF- α Antisense	CATCTTTTGGGGGAGTGCCT
mmu-GAPDH Sense	CAGGTTGTCTCCTGCGACTT
mmu-GAPDH Antisense	TATGGGGGTCTGGGATGGAA
hsa-miR-301a Sense	GCAGTGCAATAGTATTGTCAAAGC
hsa-miR-301b Sense	GCAGTGCAATGATATTGTCAAAGC
hsa-MYB Sense	CACAGAACCACACATGCAGC
hsa-MYB Antisense	GGCAGAGATGGAGTGGAGTG
hsa-IL-4 Sense	TCTTCCTGCTAGCATGTGCC
hsa-IL-4 Antisense	TGTTACGGTCAACTCGGTGC
hsa-GAPDH Sense	TGGTATCGTGGAAGGACTCA
hsa-GAPDH Antisense	CCAGTAGAGGCAGGGATGAT

Supplementary Table 3. Primers designed for luciferase reporter construct (WT c-Myb 3'UTR or Mutant c-Myb 3' UTR) containing XbaI (Sense) or FseI (Antisense) restriction sites.

ID	Primer Sequences (5'-3')
mmu-pGL3-Luc c-Myb Sense	CGAGTCTAGAGGAGAAATGTGTTCGCTGC
mmu-pGL3-Luc c-Myb Antisense	GATCGGCCGGCCGGAAGTATGTAAAATAAGAGG
mmu-pGL3-Luc c-Myb Mutant Sense	AGAGCCGTGACGCTTTTTCTTTTTTTGGGAG
mmu-pGL3-Luc c-Myb Mutant Antisense	AAGCGTCACGGCTCTTTTATAAATCGACAATAAC